Low-complexity stochastic modeling of spatially evolving flows

By W. Ran†, A. Zare†, M. J. P. Hack AND M. R. Jovanović†

Low-complexity approximations of the Navier-Stokes (NS) equations are commonly used for analysis and control of turbulent flows. In particular, stochastically forced linearized models have been successfully employed to capture structural and statistical features observed in experiments and direct simulations. In this work, we utilize stochastically forced linearized NS equations and the parabolized stability equations to study the dynamics of flow fluctuations in transitional boundary-layers. The parabolized model can be used to efficiently propagate statistics of stochastic disturbances into statistics of velocity fluctuations. Our study provides insight into interactions of slowly varying base flow with streamwise streaks and Tollmien-Schlichting waves. It also offers a systematic, computationally efficient framework for quantifying the influence of stochastic excitation sources (e.g., free-stream turbulence and surface roughness) on velocity fluctuations in weakly non-parallel flows.

1. Introduction

Nonlinear dynamical models that are based on the Navier-Stokes (NS) equations typically have a large number of degrees of freedom, a property which makes them unsuitable for analysis, optimization, and control design. The existence of coherent structures in wall-bounded shear flows (Smits, McKeon & Marusic 2011) has inspired the development of data-driven techniques for reduced-order modeling of the NS equations. However, the identified modes in nonlinear reduced-order models can be crucially altered by control actuation and sensing, which gives rise to nontrivial challenges for model-based control design (Noack, Morzyński & Tadmor 2011).

In contrast, linearized models of the NS equations around mean-velocity are well-suited for analysis and synthesis using tools of modern robust control. Linearized models subject to stochastic excitation, have been employed to replicate structural and statistical features of transitional Farrell & Ioannou (1993); Bamieh & Dahleh (2001); Jovanovic & Bamieh (2005) and turbulent Hwang & Cossu (2010); Moarref & Jovanovic (2012); Zare *et al.* (2016*b*) wall-bounded shear flows. However, most studies have focused on parallel flow configurations in which translational invariance allows for the decoupling of the dynamical equations across streamwise and spanwise wavenumbers. This offers significant computational advantages for analysis, optimization, and control.

In the flat-plate boundary layer, streamwise and normal inhomogeneity lead to a temporal eigenvalue problem for PDEs with two spatial variables. Previously, tools from sparse linear algebra and iterative schemes have been employed to analyze the spectra of the governing equations and provide insight into the dynamics of transitional flows (Ehrenstein & Gallaire 2005; Åkervik *et al.* 2008; Paredes 2014). Attempts have

† Department of Electrical and Computer Engineering, University of Minnesota

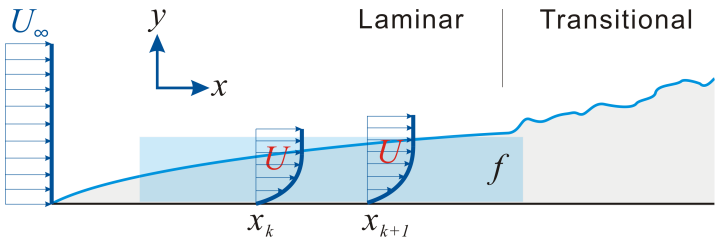

FIGURE 1: Geometry of a transitional boundary-layer flow subject to stochastic forcing.

also been made to conduct non-modal analysis of spatially evolving flows including transient growth (Åkervik *et al.* 2008; Monokrousos *et al.* 2010) and resolvent analysis (Jeun, Nichols & Jovanovic 2016). In spite of these successes, many challenges remain.

In the boundary-layer problem, the base flow is weakly non-parallel. This property can be utilized to separate slowly from rapidly varying scales in flow fluctuations. Parabolized Stability Equations (PSE) are obtained by neglecting the terms that scale as $O(1/Re^2)$ or smaller (Bertolotti, Herbert & Spalart 1992; Herbert 1997). PSE respect inhomogeneity in the streamwise direction but do not propagate information upstream, which makes them computationally more efficient than conventional flow simulations based on the NS equations (Hack & Moin 2015). They are thus routinely used to compute the spatial evolution of instability modes in a wide range of engineering problems.

Despite their popularity, parabolized equations have been utilized in a rather narrow context. We revisit the modeling of spatially evolving boundary-layer flow by examining the utility of such models in assessing the receptivity and quantifying the sensitivity to different types of flow disturbances. This examination lays the groundwork for a systematic, computationally efficient framework for quantifying the influence of stochastic excitation sources on velocity fluctuations in weakly non-parallel flows.

Our report is organized as follows. In Section 2, we describe stochastically forced linearization of the NS equations around Blasius boundary-layer flow and characterize the structural constraints imposed on second-order statistics of the linearized equations. In Section 3, we study the receptivity of the boundary layer to stochastic excitation using a parallel base flow assumption. We also perform a global stability analysis on the discretized model in two spatial directions. In Section 4, we adopt stochastic forcing to model the effect of excitations in the PSE. We summarize our developments in Section 5.

2. Problem formulation

The dynamics of incompressible Newtonian fluids are governed by the Navier-Stokes and continuity equations,

$$\begin{aligned} \mathbf{u}_t &= -(\mathbf{u}\cdot\nabla)\mathbf{u} - \nabla P + \frac{1}{\mathrm{Re}_0}\Delta\mathbf{u}, \\ 0 &= \nabla\cdot\mathbf{u}. \end{aligned}$$

We consider a flat-plate boundary-layer flow as presented in Figure 1, where $\mathbf{u}$ is the velocity vector, P is the pressure, ∇ is the gradient, and $\Delta = \nabla\cdot\nabla$ is the Laplacian. The Reynolds number is defined as $\mathrm{Re}_0 = U_\infty\delta_0/\nu$, where δ_0 is the initial Blasius length scale $\delta_0 = \sqrt{\nu x_0/U_\infty}$, U_∞ is the free-stream velocity, and ν is the kinematic viscosity. Spatial coordinates are non-dimensionalized by δ_0, velocities by U_∞, time by δ_0/U_∞, and pressure by ρU_∞^2, where ρ is the fluid density.

Linearization of the NS equations around the Blasius boundary-layer profile $\bar{\mathbf{u}} = [\,U(x,y)\;\; V(x,y)\;\; 0\,]^T$ yields the equations that govern the dynamics of velocity fluctuations $\mathbf{v} = [\,u\;\; v\;\; w\,]^T$ and pressure fluctuations p

$$\begin{array}{rcl} \mathbf{v}_t &=& -\,(\nabla\cdot\bar{\mathbf{u}})\,\mathbf{v} \;-\; (\nabla\cdot\mathbf{v})\,\bar{\mathbf{u}} \;-\; \nabla p \;+\; \dfrac{1}{\mathrm{Re}_0}\,\Delta\mathbf{v} \;+\; \mathbf{d}, \\ 0 &=& \nabla\cdot\mathbf{v}, \end{array} \tag{2.1}$$

where $\mathbf{d}$ is an additive zero-mean stochastic body forcing. The presence of stochastic forcing can be justified in different ways (Farrell & Ioannou 1993; Bamieh & Dahleh 2001; Jovanovic & Bamieh 2005). For our purposes, we wish to compensate for the role of the neglected nonlinear interactions by introducing stochastic sources of excitation that perturb the otherwise linearly developing velocity field.

After proper spatial discretization, the dynamics of velocity and pressure fluctuations are governed by the following evolution form

$$\begin{array}{rcl} \dot{\boldsymbol{\psi}}(t) &=& A\,\boldsymbol{\psi}(t) \;+\; B\,\mathbf{d}(t), \\ \mathbf{v}(t) &=& C\,\boldsymbol{\psi}(t), \end{array} \tag{2.2}$$

where $\boldsymbol{\psi}(t)$ is the state and $\mathbf{d}(t)$ is the stochastic forcing. The matrix A is the generator of the dynamics, the matrix C establishes a kinematic relationship between the components of $\boldsymbol{\psi}$ and the components of $\mathbf{v}$, and the matrix B specifies the way the external excitation $\mathbf{d}$ affects the dynamics (Jovanovic & Bamieh 2005).

2.1. *Second-order statistics and computation of energy amplification*

In statistical steady-state, the covariance matrix $\Phi = \lim\limits_{t\to\infty} \langle \mathbf{v}(t)\,\mathbf{v}^*(t)\rangle$ of the velocity fluctuation vector, and the covariance matrix $X = \lim\limits_{t\to\infty} \langle \boldsymbol{\psi}(t)\,\boldsymbol{\psi}^*(t)\rangle$ of the state in Eq. (2.2), are related as follows

$$\Phi \;=\; C\,X\,C^*,$$

where $*$ denotes complex-conjugate-transpose. The matrix Φ contains information about all second-order statistics of the fluctuating velocity field, including the Reynolds stresses.

When the dynamical generator A is linear and stable, the steady-state covariance of the state in Eq. (2.2) subject to zero-mean and white-in-time stochastic forcing with covariance $W = W^* \succeq 0$, i.e.,

$$\langle \mathbf{d}(t_1)\,\mathbf{d}^*(t_2)\rangle \;=\; W\,\delta(t_1 \,-\, t_2), \tag{2.3}$$

can be determined as the solution to the standard Lyapunov equation,

$$A\,X \;+\; X\,A^* \;=\; -B\,W\,B^*. \tag{2.4}$$

In Eq. (2.3), δ is the Dirac delta function. The Lyapunov equation relates the statistics of white-in-time forcing W to the state covariance X via system matrices A and B. The energy spectrum of velocity fluctuations that obey Eq. (2.2) can be computed as

$$E \;=\; \mathrm{trace}\,(C\,X\,C^*)\,. \tag{2.5}$$

3. Local and global analysis of stochastically forced linearized NS equations

In this section, we first examine the dynamics of flow fluctuations in the stochastically forced Blasius boundary-layer under a locally parallel base-flow assumption. This model will be parameterized over streamwise and spanwise wavenumbers, and allows for the

convenient assessment of the potential for amplifying TS waves and streamwise streaks. We then repeat the same exercise for the linearized NS equations around a spatially evolving base flow.

3.1. *Parallel Blasius boundary-layer flow subject to free-stream turbulence*

We perform an input-output analysis to quantify the energy amplification of velocity fluctuations subject to free-stream turbulence. This excitation is modeled as white-in-time stochastic forcing into the linearized NS equations around the parallel Blasius base flow profile, i.e., the Blasius profile evaluated at one streamwise location x_0 with no dependence on the streamwise coordinate. This choice is motivated by previous studies which show that transient growth exhibits similar trends for parallel and non-parallel boundary-layer flows (Andersson *et al.* 1999; Tumin & Reshotko 2001).

Under the assumption of a parallel base flow, translational invariance allows us to apply Fourier transform in the plate-parallel directions, which brings the state-space representation of the linearized NS around the Blasius boundary-layer profile at x_0 to

$$\begin{array}{rcl} \dot{\boldsymbol{\psi}}(\mathbf{k},t) & = & A(\mathbf{k})\,\boldsymbol{\psi}(\mathbf{k},t) \;+\; B(\mathbf{k})\,\mathbf{d}(\mathbf{k},t), \\ \mathbf{v}(\mathbf{k},t) & = & C(\mathbf{k})\,\boldsymbol{\psi}(\mathbf{k},t). \end{array} \tag{3.1}$$

Here, $\boldsymbol{\psi} = [\, v \;\; \eta \,]^T$ is the state, which contains the wall-normal velocity v and vorticity η. Equations (3.1) are parameterized by the spatial wavenumber pair $\mathbf{k} = (k_x, k_z)$ (see Jovanovic & Bamieh (2005) for the expressions of A, B, and C). We consider no-slip and no-penetration boundary conditions. The receptivity to external forcing that enters in various wall-normal locations can be evaluated by computing the energy spectrum of the velocity fluctuations. To specify the wall-normal region in which the forcing enters, we define $\mathbf{d} := f(y)\mathbf{d}_s$ where $\mathbf{d}_s$ represents the forcing from free-stream turbulence and $f(y)$ is the smooth function defined as

$$f(y) \;:=\; \frac{1}{\pi}\left(\operatorname{atan}(y - y_1) - \operatorname{atan}(y - y_2)\right). \tag{3.2}$$

Here, the parameters y_1 and y_2 determine the shape of $f(y)$. The energy amplification of the stochastically forced flow can be computed using the solution to the Lyapunov equation (2.5), with W being the covariance of the filtered stochastic forcing $\mathbf{d}$.

We present results obtained by computing the energy spectrum of stochastically excited parallel Blasius boundary-layer flow with $\mathrm{Re}_0 = 400$, i.e., the streamwise constant Blasius profile is computed at $x_0 = 400$. Here, we consider a wall-normal region of $L_y = 25$. A solenoidal white-in-time excitation is first introduced to the region in the immediate vicinity of the wall by choosing $y_1 = 0$ and $y_2 = 5$ in Eq. (3.2). Figure 2(a) shows that the energy of velocity fluctuations is most amplified at low streamwise wavenumbers ($k_x \approx 0$) with a global peak at $k_z \approx 0.42$. It is evident that the energy spectrum is dominated by streamwise elongated flow structures, with a trace of TS waves observed at $k_x \approx 0.35$. As the forcing region moves away from the wall, the amplification of streamwise elongated structures persists while the amplification of the TS waves weakens; see Figure 2(b). Furthermore, as the region of excitation moves away from the wall, energy amplification becomes weaker and the peak of the energy spectrum shifts to lower values of k_z. These observations are in agreement with the global analysis of boundary layer flow but are not reported here because of space constraints.

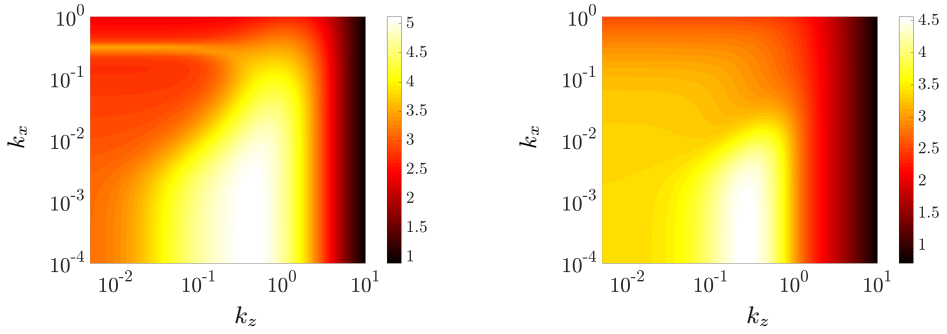

(a) (b)

FIGURE 2: Plots pf the $\log_{10}(E(\mathbf{k}))$ in the Blasius boundary-layer flow with $\mathrm{Re}_0 = 400$ subject to white-in-time stochastic excitation entering in various wall-normal regions; (a) $y_1 = 0$, $y_2 = 5$, (b) $y_1 = 5$, $y_2 = 10$ in Eq. (3.2).

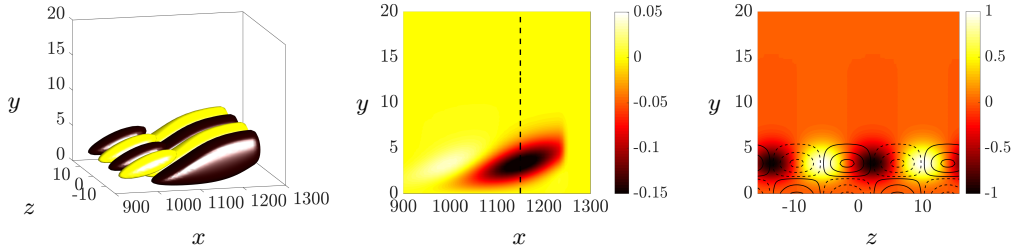

(a) streamwise velocity (b) $z = 0$ (c) $x = 1150$

FIGURE 3: Principal modes with spanwise wavenumber $k_z = 0.4$, resulting from near-wall excitation with $y_1 = 0$ and $y_2 = 5$ in Eq. (3.2). (a) Streamwise velocity component; (b) streamwise velocity at $z = 0$; (c) y-z slice of streamwise velocity (color plots) and vorticity (contour lines) at $x = 1150$.

3.2. *Global analysis of stochastically forced linearized NS equations*

We consider the linearized NS equations around a spatially evolving Blasius boundary-layer profile and introduce forcing at various wall-normal locations. The linearized NS equations around the Blasius boundary-layer flow are globally stable for the particular Reynolds number and spanwise wavenumber that we consider in this study. Thus, the steady-state covariance of the perturbation field of the stochastically forced system (2.2) can be obtained from the solution to the Lyapunov equation (2.4).

The computational region is a rectangular box with $L_x \times L_y = 900 \times 25$ and the initial Reynolds number is set to $\mathrm{Re}_0 = 400$. We consider the linearized dynamics in Eq. (2.2) with state $\boldsymbol{\psi} = [\, v \;\; \eta \,]^T$, homogenous Dirichlet boundary conditions on η and Dirichlet/Neumann boundary conditions on v, and we also introduce sponge layers in the streamwise direction (Nichols & Lele 2011; Mani 2012). Similar to Section 3.1, we assume that white-in-time stochastic forcing is filtered by the function $f(y)$ in Eq. (3.2).

Our computational experiments show that the energy amplification increases as the region of influence for the external forcing approaches the wall. This finding suggests

that perturbations entering in the vicinity of the wall are the most amplified. Figure 3(a) shows the spatial structure of the streamwise component of the principal response when white-in-time stochastic forcing enters in the vicinity of the wall ($y_1 = 0$ and $y_2 = 5$ in Eq. (3.2)). The streamwise growth of the streak structure is evident from this figure. Figure 3(b) displays the cross section of these streamwise elongated structures at $z = 0$. As Figure 3(c) demonstrates, these streaky structures are sandwiched between counter-rotating vortical motions in the cross-stream plane; and they contain alternating regions of fast- and slow-moving fluid that are slightly inclined to the wall.

4. Stochastically forced linear parabolized stability equations

Global stability analysis and direct numerical simulation of spatially evolving flows are prohibitively expensive for analysis and control purposes. On the other hand, parallel flow analysis may not be able to capture the full complexity of the spatially evolving base flow. In order to refine results from parallel flow analysis, we exploit a previously developed framework for the modeling of flow fluctuations in flat-plate boundary-layers using the PSE. In this section, we study the stochastically forced PSE in which nonlinear terms are replaced by a stochastic forcing term. A spatially evolving Blasius boundary-layer profile is considered as the base flow. The PSE can be used to efficiently advance the velocity profile downstream via a marching procedure. This also allows us to march covariance matrices downstream in a computationally efficient manner. We next provide a brief overview of the stochastically forced linear parabolized stability equations. Additional details regarding the PSE can be found in Bertolotti *et al.* (1992); Herbert (1994).

4.1. *Linear PSE*

In weakly non-parallel flows, e.g., the pre-transitional boundary-layer flow, flow fluctuations can be separated into slowly and rapidly varying components (Bertolotti *et al.* 1992). This is achieved by considering the following ansatz for the fluctuation field $\hat{\mathbf{q}} = [\, u \;\; v \;\; w \;\; p \,]^T$ in Eq. (2.1),

$$\hat{\mathbf{q}}(x, y, z, t) \;=\; \mathbf{q}(x, y)\, \chi(x, z, t),$$
$$\chi(x, z, t) \;=\; \exp\left(\mathrm{i}\,\theta(x) \,+\, \mathrm{i}\,k_z\, z \,-\, \mathrm{i}\,\omega\, t\right), \qquad \theta(x) \;=\; \int_{x_0}^{x} \alpha(\zeta)\, \mathrm{d}\zeta,$$

where $\mathbf{q}(x, y)$ and $\chi(x, z, t)$ are the shape and phase functions, k_z and ω are the spanwise wavenumber and temporal frequency, and $\alpha(x)$ is the streamwise varying generalization of the wavenumber (Bertolotti *et al.* 1992). The ambiguity arising from the streamwise variation of both $\mathbf{q}$ and α is resolved by imposing the condition $\int_{\Omega_y} \mathbf{q}^* \mathbf{q}_x \, \mathrm{d}y = 0$ (Bertolotti *et al.* 1992). The PSE approximation assumes the streamwise variation of $\mathbf{q}$ and α as sufficiently small to neglect $\mathbf{q}_{xx}$, α_{xx}, $\alpha_x \mathbf{q}_x$, and their higher order derivates with respect to x. The stochastically forced linear PSE thus take the form

$$L\,\mathbf{q} \,+\, M\,\mathbf{q}_x \,+\, \alpha_x\, N\,\mathbf{q} \;=\; \mathbf{d}, \tag{4.1}$$

where expressions for matrices L, M and N can be found in Herbert (1994).

In what follows, we use the PSE to propagate the spatially evolving state covariance,

$$X(x) \;=\; \left\langle \mathbf{q}(x)\, \mathbf{q}^*(x) \right\rangle,$$

via the discretized Lyapunov equation

$$X_{k+1} \;=\; \bar{A}_{k+1}\, X_k\, \bar{A}_{k+1}^* \;+\; \bar{B}\, \Omega_{k+1} \bar{B}^*. \tag{4.2}$$

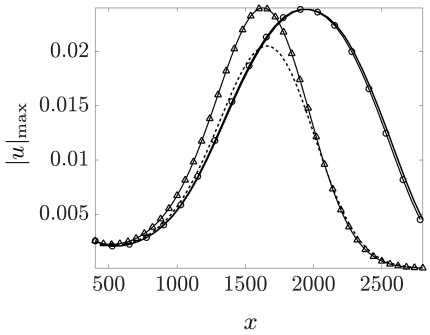

FIGURE 4: Amplitude of TS waves at $\omega = 0.0344$ in a flat-plate boundary layer flow; nonlinear PSE (solid), linear PSE without forcing (dashed), linear PSE with white forcing ($\triangle$), and linear PSE with colored forcing designed using the procedure explained in Section 4.2 ($\bigcirc$).

Here, $\langle\cdot\rangle$ is the expectation operator over various realizations of stochastic forcing, the subscript k identifies the streamwise location, and Ω represents the covariance of the white stochastic disturbance $\mathbf{d}$. The dynamical matrix $\bar{A}$ and the input matrix $\bar{B}$ result from a rearrangement of the stochastically forced linear PSE in Eq. (4.1) with a constant streamwise wavenumber α,

$$\mathbf{q}_x \;=\; \underbrace{(-M^{-1}L)}_{\bar{A}}\,\mathbf{q} \;+\; \underbrace{(-M^{-1})}_{\bar{B}}\,\mathbf{d}.$$

These equations provide a good approximation of perturbations with slowly varying streamwise wavenumbers Towne (2016). The streamwise dependence of our equations follows from the dependence of the state $\mathbf{q}$, and matrices L and M on the streamwise location x_k. Propagation of the state covariance X_k using Eq. (4.2) offers significant computational advantage over computation of the covariance from the ensemble average of many stochastic simulations.

We next consider the streamwise evolution of a two-dimensional TS wave and compare results obtained using the stochastically forced linear PSE, the linear PSE, and the nonlinear PSE. This case study was considered in Bertolotti *et al.* (1992) to demonstrate the shortcomings of linear PSE compared to nonlinear PSE.

4.2. *Streamwise evolution of a two-dimensional TS wave*

We study the streamwise evolution of a two-dimensional TS wave ($k_z = 0$) with an initial amplitude of 2.5×10^{-3} and the non-dimensional frequency $\omega = 0.0344$. All computations are initialized at $x_0 = 400$, with the streamwise wavenumber α and shape function corresponding to the TS-mode, which results from the spatial Orr-Sommerfeld/Squire problem at x_0. The initial Reynolds number is 400 and the computational domain is $L_x \times L_y = 2400 \times 60$ with homogenous Dirichlet boundary conditions applied in the wall-normal direction. We have conducted 400 simulations of stochastically forced linear PSE in Eq. (4.1), with different realizations of white stochastic forcing. As described in Section 3.1, we filter the stochastic forcing using the function $f(y)$ in Eq. (3.2) with $y_1 = 0$ and $y_2 = 10$. The resulting velocity profiles and covariances are compared with the result of linear and nonlinear PSE under the same parameter space and initial conditions.

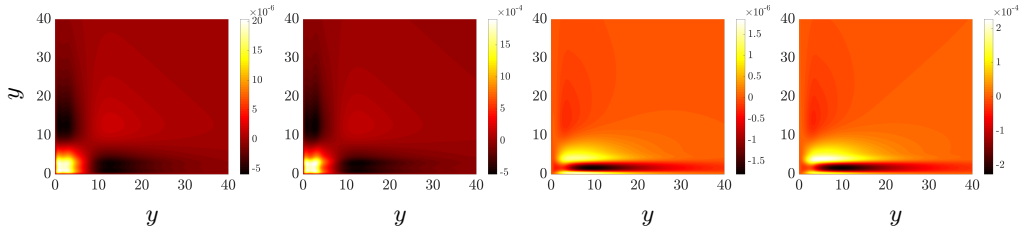

(a) X_{uu}, nonlinear PSE (b) X_{uu} (c) X_{uv}, nonlinear PSE (d) X_{uv}

FIGURE 5: Velocity covariance matrices at $x = 2800$ resulting from simulation of the nonlinear PSE (a, c) and from propagation of the discrete Lyapunov equation (4.2) (b, d) in Blasius boundary-layer flow with TS mode initialization. (a, b) The streamwise correlation X_{uu}, and (c, d) the streamwise/wall-normal cross correlation matrix X_{uv}.

Figure 4 shows the peak amplitude of the streamwise velocity component of the TS wave. Relative to nonlinear PSE, linear PSE with and without white stochastic forcing yields inaccurate predictions of the streamwise location of the peak. Figure 5 shows the streamwise covariances and the streamwise/wall-normal cross-correlation matrices at the outflow ($x = 2800$), which result from simulation of nonlinear PSE and propagation of Eq. (4.2). The outflow velocity covariances from white stochastically forced linear PSE capture the essential trends observed in the results from nonlinear PSE. However, it is not feasible to exactly match velocity correlations and growth trends with white stochastic excitation of the linear PSE. Thus it is necessary to use colored stochastic forcing. As an example, we consider a forcing field which is correlated in the streamwise direction but uncorrelated in the wall-normal direction. This allows us to better predict the location of the peak amplitude in Figure 4. To obtain this colored forcing, we first use X_k and X_{k+1} resulting from nonlinear PSE to compute the covariance $Z_k := \bar{B}\,\Omega_k \bar{B}^*$. This covariance corresponds to a spatially correlated process in the streamwise direction and is thus not necessarily positive semi-definite. We then project these forcing correlations onto the positive-definite cone to achieve uncorrelated noise in the wall-normal direction. The result of incorporating this colored (in the streamwise direction) forcing is also shown in Figure 4. Clearly, the peak amplitude resulting from this model matches the curve from nonlinear PSE simulations.

To further evaluate the performance of this model, we examine the error in matching the full state covariance matrix X and the amplitude of the streamwise velocity profile $|u|$ as a function of the streamwise location x; see Figure 6(a). Although we are able to reliably approximate the location of the peak, exact amplitudes and velocity covariances cannot be achieved. Figures 6(b) and 6(c) show the amplitude of the streamwise velocity $|u|$ at the location with highest error ($x = 1840$) and the outflow ($x = 2800$), respectively. While the profiles perfectly match for $y < 30$, the profiles resulting from linear PSE with colored forcing experience significant deviations in the outer flow.

5. Concluding remarks

In the present study, we have utilized stochastically forced linearized NS equations and stochastically forced linear PSE to study the dynamics of flow fluctuations in the Blasius

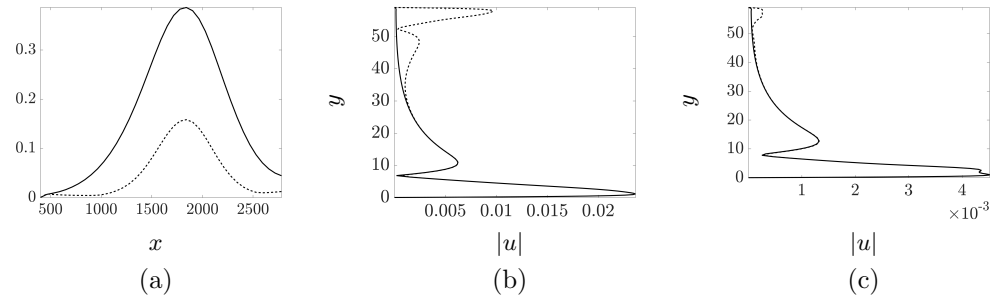

FIGURE 6: (a) Relative error in matching the amplitude of streamwise velocity (solid) and in matching the state covariance $X(x)$ (dashed) using the linear PSE with colored forcing in the spatial evolution of a 2-D TS wave at $\omega = 0.0344$; the amplitude of the streamwise component of TS waves at (a) $x = 1840$ and (b) $x = 2800$, resulting from nonlinear PSE (solid) and linear PSE with colored forcing (dashed).

boundary-layer. In particular, we have examined the receptivity of the spatially evolving Blasius boundary-layer flow to free-stream disturbances which we model as stochastic excitations that enter at specific wall-normal locations. We also incorporate stochastic forcing into the linear PSE to study the streamwise evolution of TS waves. While white stochastic excitation is unable to improve predictions relative to the conventional linear PSE, we achieve better predictions of transient peaks using colored forcing. The predictive power of our approach can be further improved by utilizing recently developed theoretical framework for identifying spatio-temporal spectrum of stochastic excitation sources (Zare *et al.* 2016*a*,*b*). The problem of employing such a framework in order to recover partially observed statistical signatures of spatially evolving flows via low-complexity stochastic models will be studied in our future work.

Acknowledgments

We thank Prof. P. Moin for his interest in our work and for providing us with the opportunity to participate in the CTR Summer Program; Prof. P. J. Schmid and Prof. J. W. Nichols for useful discussions; and Dr. A. Towne for his comments on an earlier draft of this report. Partial support from the National Science Foundation under Award CMMI 1363266, the Air Force Office of Scientific Research under Award FA9550-16-1-0009 is gratefully acknowledged. The University of Minnesota Supercomputing Institute is acknowledged for providing computing resources.

REFERENCES

ÅKERVIK, E., EHRENSTEIN, U., GALLAIRE, F. & HENNINGSON, D. S. 2008 Global two-dimensional stability measures of the flat plate boundary-layer flow. *Eur. J. Mech. B* **27**, 501–513.

ANDERSSON, P., BERGGREN, M. & HENNINGSON, D. 1999 Optimal disturbances and bypass transition in boundary layers. *Phys. Fluids* **11**, 134–150.

BAMIEH, B. & DAHLEH, M. 2001 Energy amplification in channel flows with stochastic excitation. *Phys. Fluids* **13**, 3258–3269.

BERTOLOTTI, F. P., HERBERT, T. & SPALART, P. R. 1992 Linear and nonlinear stability of the Blasius boundary layer. *J. Fluid Mech.* **242**, 441–474.

Ehrenstein, U. & Gallaire, F. 2005 On two-dimensional temporal modes in spatially evolving open flows: the flat-plate boundary layer. *J. Fluid Mech.* **536**, 209–218.

Farrell, B. F. & Ioannou, P. J. 1993 Stochastic forcing of the linearized Navier-Stokes equations. *Phys. Fluids* **5**, 2600–2609.

Hack, M. J. P. & Moin, P. 2015 Towards modeling boundary layer transition in large-eddy simulations. *Annual Research Briefs*, Center for Turbulence Research, Stanford University, pp. 137–144.

Herbert, T. 1994 Parabolized stability equations. In *Special Course on Progress in Transition Modelling*, chap. 4, pp. 1–34. AGARD Rep., No. 793.

Herbert, T. 1997 Parabolized stability equations. *Annu. Rev. Fluid Mech.* **29**, 245–283.

Hwang, Y. & Cossu, C. 2010 Linear non-normal energy amplification of harmonic and stochastic forcing in the turbulent channel flow. *J. Fluid Mech.* **664**, 51–73.

Jeun, J., Nichols, J. W. & Jovanovic, M. R. 2016 Input-output analysis of high-speed axisymmetric isothermal jet noise. *Phys. Fluids* **28**, 047101.

Jovanovic, M. R. & Bamieh, B. 2005 Componentwise energy amplification in channel flows. *J. Fluid Mech.* **534**, 145–183.

Mani, A. 2012 Analysis and optimization of numerical sponge layers as a nonreflective boundary treatment. *J. Comput. Phys.* **231**, 704–716.

Moarref, R. & Jovanovic, M. R. 2012 Model-based design of transverse wall oscillations for turbulent drag reduction. *J. Fluid Mech.* **707**, 205–240.

Monokrousos, A., Åkervik, E., Brandt, L. & Henningson, D. S. 2010 Global three-dimensional optimal disturbances in the blasius boundary-layer flow using time-steppers. *J. Fluid Mech.* **650**, 181–214.

Nichols, J. W. & Lele, S. K. 2011 Global modes and transient response of a cold supersonic jet. *J. Fluid Mech.* **669**, 225–241.

Noack, B. R., Morzyński, M. & Tadmor, G. 2011 *Reduced-order modelling for flow control*, *CISM Courses and Lectures*, vol. 528. Springer.

Paredes, G. P. 2014 *Advances in global instability computations: from incompressible to hypersonic flow.* PhD Thesis, Technical University of Madrid.

Smits, A. J., McKeon, B. J. & Marusic, I. 2011 High-Reynolds number wall turbulence. *Annu. Rev. Fluid Mech.* **43**, 353–375.

Towne, A. 2016 *Advancements in jet turbulence and noise modeling: accurate one-way solutions and empirical evaluation of the nonlinear forcing of wavepackets.* PhD Thesis, California Institute of Technology.

Tumin, A. & Reshotko, E. 2001 Spatial theory of optimal disturbances in boundary layers. *Phys. Fluids* **13**, 2097–2104.

Zare, A., Chen, Y., Jovanovic, M. R. & Georgiou, T. T. 2016*a* Low-complexity modeling of partially available second-order statistics: theory and an efficient matrix completion algorithm. *IEEE Trans. Automat. Control* doi:10.1109/TAC.2016.2595761; also arXiv:1412.3399.

Zare, A., Jovanovic, M. R. & Georgiou, T. T. 2016*b* Color of turbulence. *J. Fluid Mech.* (To appear); also arXiv:1602.05105.